Chemical Engineering Communications

ISSN: 0098-6445 (Print) 1563-5201 (Online) Journal homepage: http://www.tandfonline.com/loi/gcec20

Nonlinear control of a batch crystallizer

J. R. Corriou & S. Rohani

To cite this article: J. R. Corriou & S. Rohani (2002) Nonlinear control of a batch crystallizer, Chemical Engineering Communications, 189:10, 1415-1436, DOI: 10.1080/00986440214062

To link to this article: http://dx.doi.org/10.1080/00986440214062

Chem. Eng. Comm., 189: 1415–1436, 2002

0098-6445/02 $12.00 + .00
DOI: 10.1080/00986440290012834

NONLINEAR CONTROL OF A BATCH CRYSTALLIZER

J. R. CORRIOU

LSG – CNRS – ENSIC,
Nancy, France

S. ROHANI

Department of Chemical and Biochemical Engineering,
The University of Western Ontario,
London, Ontario, Canada

A nonlinear geometric feedback controller with and without state estimation (the extended continuous-discrete Kalman filter) is developed and applied to a 0.027 m^3 potash alum batch crystallizer. The manipulated variable is the temperature of the inlet cooling water supplied to the jacket of the crystallizer, and the controlled variable is the supersaturation. It is shown that the controller eliminates the large initial peak in the supersaturation (which results in excessive nucleation) and maintains the supersaturation at its set-point, provided that the manipulated variable does not reach its constraints. The controller performs well with only two measured states (the crystallizer temperature and the solute concentration) and results in larger terminal crystal mean size in comparison with natural cooling and linear cooling policies with fines dissolution.

Keywords: Nonlinear geometric control; Extended Kalman filter; Batch cooling crystallization; Potash alum

INTRODUCTION

Batch crystallization is an important separation and processing unit operation in chemical and pharmaceutical industries. In the operation of batch crystallizers the purity, size distribution, and shape of the final

Address correspondence to S. Rohani, Department of Chemical and Biochemical Engineering, University of Western Ontario, London, ON, Canada N6A 5B9. E-mail: rohani@uwo.ca

product must be controlled, despite an inherently time-varying supersaturation level. In the past, many researchers have addressed this control problem for cooling batch crystallizers in particular. These numerous studies can be divided into two main categories: programmed or optimal cooling policies and control based on fines dissolution. It is well known that significant improvement in product quality may be realized by forcing the crystallizer to follow a programmed or an optimal cooling policy in comparison to natural or linear cooling. In the first category of studies, among many others, is the work of Jones and Mullin (1974), Mayrhofer and Nyvlt (1988), Miller and Rawlings (1994), and Sheik and Jones (1997). The programmed or optimal cooling policy, although effective theoretically, is essentially an open-loop control policy and therefore incapable of responding to variations in feed composition from batch to batch and other external disturbances. The second category of study deals with fines dissolution. Jones and Chianese (1987) used a constant rate of fines dissolution during the entire batch operation. Rohani et al. (1990), however, applied a feedback controller in conjunction with a fines suspension density meter to dissolve the excess nuclei during the operation of a batch crystallizer. Later on, Rohani and Bourne (1990) used an adaptive controller to demonstrate the efficacy of the feedback control of fines suspension density.

In the present work, we will develop a nonlinear feedback controller to maintain the driving force of the crystallization, namely the supersaturation. We will demonstrate that the proposed controller in conjunction with the extended Kalman filter is capable of maintaining the supersaturation by measuring only two state variables, namely the crystallizer temperature and the solute concentration.

THE CRYSTALLIZER MODEL

Figure 1 shows the schematics of a batch crystallizer with its cooling jacket. The crystal population density in the absence of aggregation and breakage and for size-independent growth rate is

$$\frac{\partial n(L,t)}{\partial t} + G(t)\frac{\partial n(L,t)}{\partial L} = 0, \tag{1}$$

with $n(L,0) = n_0$ representing the initial population density and $n(0,t) = B(t)/G(t)$ representing the population density of zero size nuclei. The kth moment of the population density can be obtained from Equation (1):

$$\frac{dm_k(t)}{dt} = 0^k B(t) + kG(t)m_{k-1}(t), \tag{2}$$

with $m_k(0) = m_{k0}$.

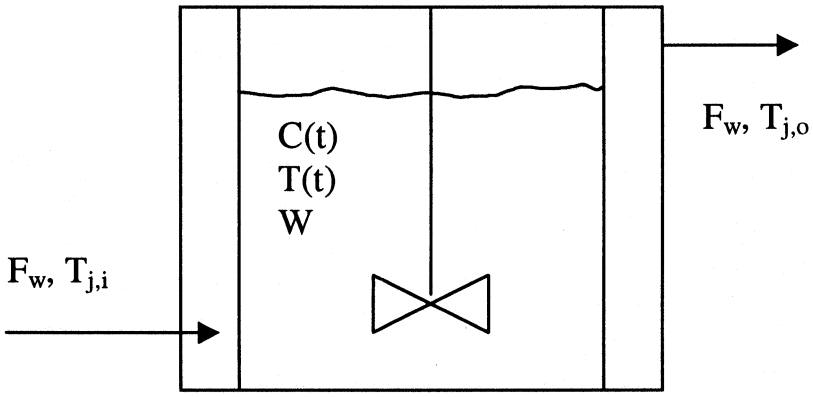

Figure 1. Schematics of the cooling batch crystallizer with the cooling jacket.

The solute mass balance is

$$\frac{dC(t)}{dt} = -\rho_c k_v \frac{dm_3(t)}{dt}, \tag{3}$$

with $C(0) = C_0$ as the initial concentration of the solute. The energy balance on the crystallizer content is

$$\frac{dh(t)}{dt} = \dot{q}(t), \tag{4}$$

where $h(t)$ is the total enthalpy content of the crystallizer,

$$h(t) = W\big[T(t) - T_{ref}\big]\big\{[1 + C(t)]c_p + m_3(t)\rho_c k_v c_{p,c}\big\}, \tag{5}$$

and $\dot{q}(t)$ is the rate of heat removal from the crystallizer,

$$\dot{q}(t) = UA\big[T(t) - T_j(t)\big]. \tag{6}$$

Substitution of Equations (3), (5), and (6) in Equation (4) and simplifying the resulting equation results in

$$\frac{dT(t)}{dt} = \left\{\frac{UA\big[T(t) - T_j(t)\big]}{W} - \rho_c k_v \frac{\Delta H}{[C(t) - C^*]} \frac{dm_3(t)}{dt}\right\} \Big/ \big\{c_p[1 + C(t)] + c_{p,c}\ \rho_c k_v m_3(t)\big\}, \tag{7}$$

with $T(0) = T_0$ as the crystallizer temperature at $t = 0$.

The energy balance on the cooling jacket is:

$$\frac{dT_j(t)}{dt} = \frac{F_w}{V_j}\left[T_{j,i}(t) - T_{j,o}(t)\right] + \frac{UA}{\rho_w V_j c_{p,w}}\left[T(t) - T_j(t)\right], \tag{8}$$

where $T_{j,o} = T_j$ at high cooling water flow rates or $T_{j,o} = 2T_j - T_{j,i}$ at low flow rates and $T_j(0) = T_{j0}$.

The saturation concentration of the solute is usually given as a function of the temperature:

$$C^*(t) = c_0 + c_1 T + c_2 T^2, \tag{9}$$

and the nucleation and growth rates are expressed in terms of the supersaturation $\Delta C = C - C^*$:

$$B(t) = b_o k_v \rho_c m_3(t)[\Delta C(t)]^{b_1} \frac{1 + C(t)}{\rho_s} \exp\left[-\frac{E_B}{RT(t)}\right], \tag{10}$$

$$G(t) = a_0[\Delta C(t)]^{a_1} \exp\left[-\frac{E_G}{RT(t)}\right]. \tag{11}$$

The physical constants are listed in Table I.

NONLINEAR GEOMETRICAL CONTROL

Some books in the literature are partially or totally dedicated to nonlinear geometrical control. Among them, Isidori (1995), Nijmeijer and

Table I Operating Conditions and Physical Constants Used in the Model (Akoglu et al., 1984)

c*	$= 4.1636 - 0.031\mathrm{T} + 5.85^{*}10^{-5}\mathrm{T}^2$
B	$= 1.15^{*}10^{28}\ \mathrm{k_v}\ \rho_c\ \mathrm{m_3}\ (\Delta\mathrm{C})^{2.1}\ \exp[-\frac{10^5}{RT}]\ \frac{1+C}{\rho_s}$
G	$= 39.94\ (\Delta\mathrm{C})^{1.38}\ \exp[-\frac{3.2^{*}10^4}{RT}]$
c_{pc}	= 840
c_{pw}	= 3800
F_w	$= 10^{-3}$
k_v	= 1
UA	= 800
V_j	= 0.015
W	= 27
ΔH	$= -4220$
ρ_c	= 1760
ρ_s	$= -621.32 + 5.5\,\mathrm{T}$
ρ_w	= 1000

van der Schaft (1990), Slotine and Li (1991), Khalil (1996), and Levine (1996) must be cited.

Consider a SISO (Single Input/Single Output) system affine with respect to input u of the form

$$\begin{cases} \dot{x} = f(x(t)) + g(x(t))u \\ y = h(x(t)) \end{cases}, \tag{12}$$

where $x \in R^n$ is the state vector, $u \in R$ the input vector, and $y \in R$ the output vector. $f(x)$ and $g(x)$ are vectors of functions. Note that most systems in chemical engineering belong to this class of affine systems.

Most of the following definitions or properties will be given locally in the neighborhood of a point x_0.

The relative order of the nonlinear system given by Equation (12) is defined (Hirschorn, 1979) as the smallest integer r such that

$$L_g L_f^{r-1} h(x) \neq 0, \tag{13}$$

where $L_f\, h(x)$ represents the Lie derivative of h, given the field vector f:

$$L_f h(x) = \sum_{i=1}^{n} \frac{\partial h}{\partial x_i} f_i(x). \tag{14}$$

The r first derivatives of the output of the system in Equation (12) are

$$\begin{pmatrix} \dot{y} \\ \vdots \\ y^{(r-1)} \\ y^{(r)} \end{pmatrix} = \begin{pmatrix} L_f h(x) \\ \vdots \\ L_f^{r-1} h(x) \\ L_f^r h(x) + L_g L_f^{r-1} h(x) u \end{pmatrix}. \tag{15}$$

Another important property is that the set of r fields of scalars $h(x)$, $L_f h(x), \ldots, L_f^{r-1} h(x)$ are linearly independent (Isidori, 1995) and that consequently $r \leq n$ where n is the order of the system given in Equation (12).

Normal Form of Byrnes-Isidori

Consider the nonlinear system given in Equation (12) of relative order $r \leq n$ with the change of coordinates $z = \Phi(x)$ whose r first components are:

$$\begin{pmatrix} z_1 \\ z_2 \\ \vdots \\ z_r \end{pmatrix} = \begin{pmatrix} \phi_1(x) \\ \phi_2(x) \\ \vdots \\ \phi_r(x) \end{pmatrix} = \begin{pmatrix} h(x) \\ L_f h(x) \\ \vdots \\ L_f^{r-1} h(x) \end{pmatrix}. \tag{16}$$

If r is smaller than n, it is often possible to find $(n-r)$ functions $\phi_{r+1}(x), \ldots, \phi_n(x)$ such that the vector

$$\Phi(x) = \begin{pmatrix} h(x) \\ L_f h(x) \\ \vdots \\ L_f^{r-1} h(x) \\ \phi_{r+1}(x) \\ \vdots \\ \phi_n(x) \end{pmatrix} \tag{17}$$

has a Jacobian matrix that is nonsingular. In particular, the $(n-r)$ functions $\phi_{r+1}(x), \ldots, \phi_n(x)$ are chosen such that

$$L_g \phi_i(x) = 0 \quad \forall\, r+1 \le i \le n. \tag{18}$$

If the transformed variables $z = \Phi(x)$ and their inverse $x = \Phi^{-1}(z)$, defined for all $x \in R^n$ and $z \in R^n$, are smooth mappings, they are global diffeomorphisms. If they can only be defined in the neighborhood of a point x_0 and z_0, they are local diffeomorphisms.

The normal form of Byrnes-Isidori is obtained:

$$\begin{cases} \dot{z}_1 = z_2 \\ \quad\vdots \\ \dot{z}_{r-1} = z_r \\ \dot{z}_r = b(z) + a(z)u, \\ \dot{z}_{r+1} = F_{r+1}(z) \\ \quad\vdots \\ \dot{z}_n = F_n(z) \end{cases} \tag{19}$$

together with the output equation

$$y = z_1, \tag{20}$$

where $a(z) = L_g L_f^{r-1} h\left[\Phi^{-1}(z)\right], b(z) = L_f^r h\left[\Phi^{-1}(z)\right]$, and $F_i(z) = L_f \phi_i\left(\Phi^{-1}(z)\right)\ \forall r+1 \le i \le n$.

Exact Input-State Feedback Linearization

The nonlinear system given in Equation (12) can, in some cases, be transformed into a linear controllable system (the canonical form of Brunovsky) after an appropriate change of coordinates: $z = \Phi(x)$ and a state feedback law.

Input-State Feedback Linearization when $r = n$. First, consider the nonlinear system given by Equation (12) with relative order r equal to the number of states n.

The diffeomorphism given by Equation (16) is applied to this system. It results in the normal form of Byrnes-Isidori given by Equation (19), except that the last $(n - r)$ components have disappeared. Setting the external input $v = \dot{z}_n$, the following state feedback control law is obtained:

$$u = \frac{v - b(z)}{a(z)}, \tag{21}$$

where $a(z)$ is nonzero by definition of the relative order. This transforms the normal form of Byrnes-Isidori into the canonical form of Brunovsky:

$$\begin{cases} \dot{z}_1 = z_2 \\ \dot{z}_2 = z_3 \\ \quad\vdots \quad . \\ \dot{z}_{n-1} = z_n \\ \dot{z}_n = v \end{cases} \tag{22}$$

$$y = z_1$$

Thus the nonlinear system of Equation (12) of relative order $r = n$ has been transformed into a linear and controllable closed loop system via a local diffeomorphism and the static state feedback reformulated as

$$u = \frac{v - L_f^n h(x)}{L_g L_f^{n-1} h(x)} \tag{23}$$

Input-State Feedback Linearization when $r < n$. In many cases, the system of Equation (12) has a relative order lower than the state dimension ($r < n$). Then, the problem of exact linearization in the state space is solvable if and only if there exists a function γ(x) such that the system

$$\begin{cases} \dot{x} = f(x) + g(x)u \\ y' = \gamma(x) \end{cases} \tag{24}$$

has a relative order equal to n and

$$\begin{cases} L_g L_f^i \gamma(x) & = & 0 \quad \text{for } 0 \leq i \leq n-2 \\ L_g L_f^{n-1} \gamma(x) & \neq & 0 \end{cases} . \tag{25}$$

Note that Equation (25) is equivalent to the following set of equations:

$$\begin{cases} L_g \gamma(x) & = & 0 \\ L_{ad_f^1 g} \gamma(x) & = & 0 \\ & \vdots & , \\ L_{ad_f^{n-2} g} \gamma(x) & = & 0 \\ L_{ad_f^{n-1} g} \gamma(x) & \neq & 0 \end{cases} \tag{26}$$

where

$$ad_f g(x) = [f, g](x) = \frac{\partial g}{\partial x} f(x) - \frac{\partial f}{\partial x} g(x) \quad \text{and}$$
$$ad_f^i g(x) = \left[f, ad_f^{i-1} g \right](x) \text{ for } i > 1 \tag{27}$$

Equation (26) is a consequence of the Frobenius theorem. The new output function $\gamma(x)$ exists if and only if the following conditions are satisfied:

(i) the fields of vectors

$$g(x), ad_f^1 g(x), \ldots, ad_f^{n-1} g(x)$$

are linearly independent, i.e., the matrix $[g(x) ad_f^1 g(x), \ldots, ad_f^{n-1} g(x)]$ has rank n, and

(ii) the set of fields of vectors

$$g(x), ad_f^1 g(x), \ldots, ad_f^{n-2} g(x)$$

is involutive.

Finding the new "output" implies solving the system of partial derivatives equations given by Equation (26). For the exact state-space linearization, a change of coordinates and a state feedback law are necessary. The change of coordinates is given by

$$\Phi(x) = \begin{pmatrix} \gamma(x) \\ L_f \gamma(x) \\ \vdots \\ L_f^{n-1} \gamma(x) \end{pmatrix}, \tag{28}$$

and the resulting state feedback law is

$$u = \frac{v - L_f^n \gamma(x)}{L_g L_f^{n-1} \gamma(x)}. \tag{29}$$

The system with the new "output" $\gamma(x)$ is thus a linear and controllable one, but the "output" $\gamma(x)$ is nonlinear. A complete linearization of the original system would involve a linearization of the output mapping.

Control Law for Input-Output Feedback Linearization

Assume that the system of Equation (12) has a relative order $r \leq n$ (defined and constant in the region of interest). Consider the linear and nonlinear parts of the normal form of Equation (19) as, respectively,

$$\xi = (y, \dot{y}, \ldots, y^{(r)})^T = (z_1, \ldots, z_r)^T \quad \text{and} \quad \eta = (z_{r+1}, \ldots, z_n)^T, \tag{30}$$

so that the normal form can be written as

$$\begin{cases} \dot{z}_1 &= & z_2 \\ & \vdots & \\ \dot{z}_{r-1} &= & z_r \\ \dot{z}_r &= & b(\xi, \eta) + a(\xi, \eta) u \\ \dot{\eta} &= & F(\xi, \eta) \end{cases}. \tag{31}$$

Setting $v = \dot{z}_r$, the control law is chosen as

$$u = \frac{v - b(\xi, \eta)}{a(\xi, \eta)} = \frac{v - L_f^r h}{L_g L_f^{r-1} h}, \tag{32}$$

which yields the following closed loop system:

$$\begin{aligned} \dot{\xi} &= A\xi + Bv \\ \dot{\eta} &= F(\xi, \eta), \end{aligned} \tag{33}$$

where A and B are constant matrices. The r first equations of Equation (31) correspond to a linear controllable and observable subsystem that gives to the closed loop system a linear input-output behavior

$$y^{(r)} = v \tag{34}$$

The $(n-r)$ last equations of Equation (31) correspond to unobservable states; they represent a realization of minimum order of the inverse of the system of Equation (12) and pose a stability problem. Considering that the origin is the equilibrium point, if the output y and its successive derivatives are null, the zero dynamics are defined by the solution of

$$\dot{\eta}(t) = F(0, \eta(t)), \tag{35}$$

which aims to maintain $\xi(t) = 0$, which is supposed to be the stationary point of Equation (12). The control law is then

$$u = \frac{-b(0, \eta(t))}{a(0, \eta(t))}. \tag{36}$$

The nonlinear system of Equation (12) is minimum phase if the zero dynamics are asymptotically stable around a stationary operating point. This can be extended to a reference trajectory y_R by subsequent modification of vector ξ. In that case, the error $e(t) = y(t) - y_R(t)$ must satisfy the following equation:

$$e^{(r)}(t) + \alpha_{r-1} e^{(r-1)}(t) + \cdots + \alpha_1 e^{(1)}(t) + \alpha_0 e(t) + \rho \int_0^t e \, d\delta = 0, \tag{37}$$

where $\alpha_{r-1}, \ldots, \alpha_0, \rho$ are chosen such that the polynomial

$$s^{r+1} + \alpha_{r-1} s^r + \cdots + \alpha_1 s^2 + \alpha_0 s + \rho \tag{38}$$

is Hurwitz. Since $e = y - y_R$, $e^{(1)} = y^{(1)} - y_R{}^{(1)}, \ldots,$ and $e^{(r)} = y^{(r)} - y_R{}^{(r)} = v - y_R{}^{(r)}$, Equation (37) can be solved with respect to v to deduce the control law:

$$v = y_R^{(r)} - \alpha_{r-1} e^{(r-1)}(t) - \cdots - \alpha_1 e^{(1)}(t) - \alpha_0 e(t) - \rho \int_0^t e \, d\delta. \tag{39}$$

Then the error vector converges exponentially towards zero.

APPLICATION OF THE NONLINEAR CONTROL TO A BATCH CRYSTALLIZER

The nonlinear control discussed above was applied to a batch cooling potash alum crystallizer (Rohani et al., 1990). The crystallizer was a

jacketed vessel charged with a potash alum solution (saturated at 313 K) containing 27 kg of solvent (water). The operating conditions are given in Table I.

The cooling water inlet temperature to the jacket $T_{j,in}$ was selected as the manipulated variable, u, and the supersaturation ΔC as the controlled variable, y. The manipulated variable is allowed to vary between 263.15 K and 353.15 K and is constrained between these two values. Eight state variables were defined: the solute concentration, C, the first five leading moments of the population density, m_o to m_4, the crystallizer and the jacket temperature, T and T_j.

Equations (2), (3), (7), and (8) using Equations (9) to (12) may be written in state space form

$$\begin{cases} \dot{x}_1 = 3\rho_c k_v a_o \left(x_1 - c_o - c_1 x_7 - c_2 x_7^2\right)^{a_1} \exp\left(-\frac{E_G}{R x_7}\right) x_4 \\ \dot{x}_2 = b_o k_v \rho_c x_5 \left(x_1 - c_o - c_1 x_7 - c_2 x_7^2\right)^{b_1} \exp\left(-\frac{E_B}{R x_7}\right) \frac{1+x_1}{r_o + r_1 x_7} \\ \dot{x}_3 = a_o \left(x_1 - c_o - c_1 x_7 - c_2 x_7^2\right)^{a_1} \exp\left(\frac{E_G}{R x_7}\right) x_2 \\ \dot{x}_4 = 2a_o \left(x_1 - c_o - c_1 x_7 - c_2 x_7^2\right)^{a_1} \exp\left(\frac{E_G}{R x_7}\right) x_3 \\ \dot{x}_5 = 3a_o \left(x_1 - c_o - c_1 x_7 - c_2 x_7^2\right)^{a_1} \exp\left(\frac{E_G}{R x_7}\right) x_4 \\ \dot{x}_6 = 4a_o \left(x_1 - c_o - c_1 x_7 - c_2 x_7^2\right)^{a_1} \exp\left(\frac{E_G}{R x_7}\right) x_5 \\ \dot{x}_7 = \frac{1}{W\left[c_{p,w}(1+x_1) + \rho_c k_v c_{p,c} x_5\right]} \left[UA(x_8 - x_7)\right. \\ \qquad \left. \times -3W\rho_c k_v \Delta H a_o \left(x_1 - c_o - c_1 x_7 - c_2 x_7^2\right)^{a_1 - 1} \exp\left(\frac{E_G}{R x_7}\right)\right] x_4 \\ \dot{x}_8 = \frac{F_w}{V_j}(u - x_8) + \frac{UA}{\rho_w V_j c_{p,w}}(x_7 - x_8) \\ y = x_1 - c_0 - c_1 x_7 - c_2 x_7^2 \end{cases} \tag{40}$$

Note that the system of Equation (40) is affine with respect to the manipulated variable u and thus can be written as in Equation (12). The vectors f and g can easily be deduced from Equation (40).

In order to determine the relative order, we find that $L_g h(x) = 0$ and

$$L_g L_f h(x) = \frac{\partial L_f h(x)}{\partial x_8} g_8 = (-c_1 - 2c_2 x_7) \frac{UA}{W\left[(1 + x_1)c_{p,w} + \rho_c k_v x_5 c_{p,c}\right]} g_8 \neq 0$$

Thus the relative order r of the system is in general equal to 2. However, there exists a singularity when the first factor of the previous

expression becomes equal to 0 for $x_2 = 264.96\,\text{K}$. When the crystallizer temperature falls below this value, in fact the minimum inlet cooling temperature is already imposed and the valve is completely closed; thus it remains in this position.

The application of input-state feedback linearization remains extremely difficult to realize in the cases where the number of state equations n is greater than 2. Thus for our case, input-output linearization is applied. The control law that ensures a linear input-output behavior is defined as

$$u = \frac{v - (L_f^2 h(x) - y_R^{(2)}) - \theta_1\left(L_f h(x) - y_R^{(1)}\right) - \theta_0(h(x) - y_R)}{L_g L_f h(x)}, \tag{41}$$

where y_R is the reference trajectory and v is the external input given by a PI controller. θ_i are parameters defined by the user so that the resulting closed-loop behavior presents adequate properties of robustness and performance. In addition to $L_g L_f h(x)$, the Lie derivatives of interest are

$$L_f h(x) = f_1 + (-d_2 - 2d_3 x_7) f_7 \qquad L_f^2 h(x) = \sum_{i=1,4,5,7,8} \frac{\partial L_f h}{\partial x_i} f_i.$$

Two cases are studied: first it is assumed that all states (x_1 to x_8) are known, and in the second case it is assumed that only the crystallizer temperature and the solute concentration are measured and the other states are estimated.

Control with All States Known

It is assumed that initially seed crystals of the same size $L_S = 100\,\mu\text{m}$ with a total mass $m = 10^{-3}\,\text{kg}$ are present. The initial values of all moments are:

$$\begin{aligned} m_{00} &= \frac{m}{\rho_c k_v L_s^3 W}, \\ m_{io} &= m_{i-1} L_s \quad \forall 1 \le i \le 4. \end{aligned} \tag{42}$$

The set-point is chosen as 0.015 kg/kg solvent. In order to avoid large transients of the manipulated variable, the set-point is filtered by a second-order continuous transfer function with a damping coefficient 1.2 and a time constant 50 s, thus resulting in the reference trajectory. The tuning parameters of the control law are taken as $\theta_0 = 0.001$, $\theta_1 = 0.1$, and

the external input is the output of a PI controller with proportional gain 0.0002 and an integral time constant 10 s, while the input of the controller is the error between the reference trajectory and the output. The initial crystallizer temperature is 313 K.

Figure 2 shows the profiles of the inlet jacket temperature, the jacket temperature, and the crystallizer temperature. Note that the crystallizer temperature initially increases in order to decrease the supersaturation peak (see Figure 3). Supersaturation is brought to its set-point and is well controlled up to time 2600 s. At this time, the inlet jacket temperature reaches its lower constraint (263 K, see Figure 2), which means that the maximum cooling is imposed to the crystallizer and supersaturation control is lost. Despite the loss of control after 2600 s, the final crystal mean size (m_5/m_4) shown in Figure 4 reaches 780 μm, which is larger than as reported by Rohani et al. (1990): 529 μm and 640 μm for natural cooling and linear cooling with fines dissolution, respectively. Figure 5 shows the product yield, which assumes a sigmoidal shape: at the beginning, the yield is very low; after about 1500 s, it increases very rapidly, and then at a slower rate after 2600 s.

The simulation results presented in Figures 2 to 5 were obtained assuming that all the states are perfectly known. This assumption, however, calls for a precise particle size analyzer to determine the first five leading moments of the population density, which is a formidable task. Therefore, in the next section we will use an extended Kalman filter,

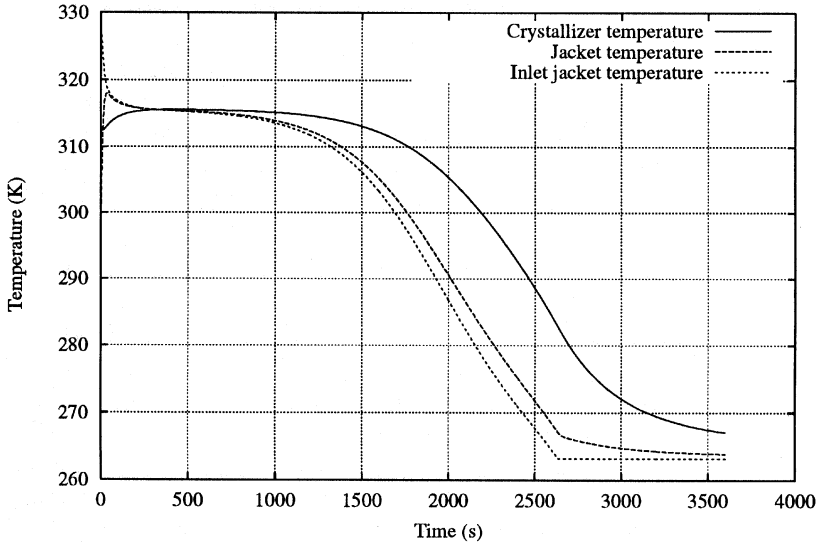

Figure 2. The supersaturation and its set-point using the nonlinear controller with complete knowledge of state variables.

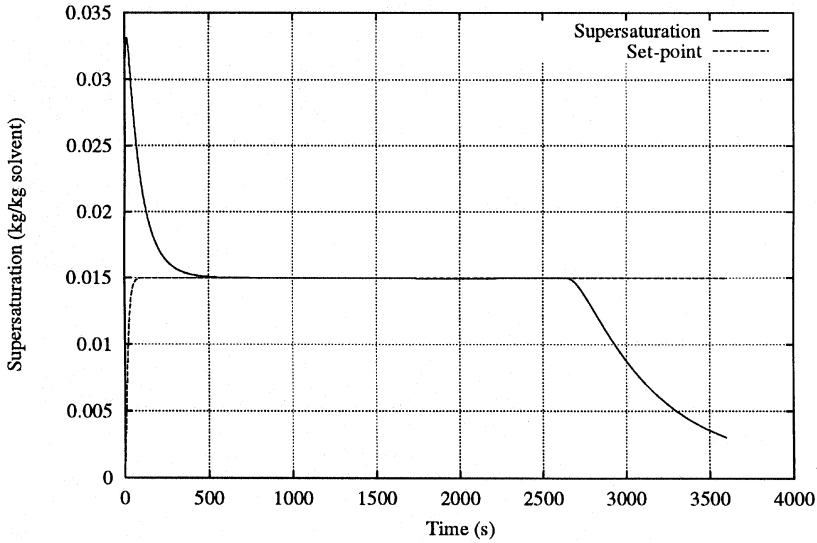

Figure 3. The crystallizer, jacket, and inlet cooling water temperatures using the nonlinear controller with complete knowledge of state variables.

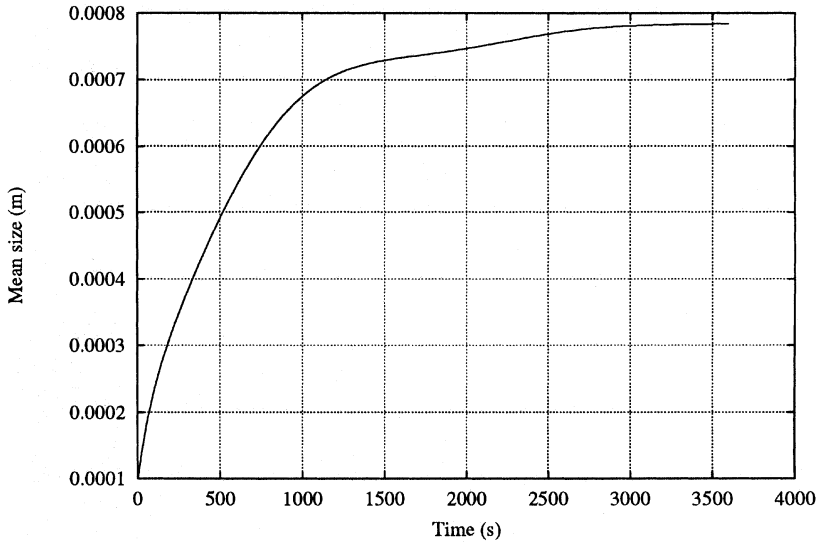

Figure 4. The terminal crystal mean-size using the nonlinear controller with complete knowledge of state variables.

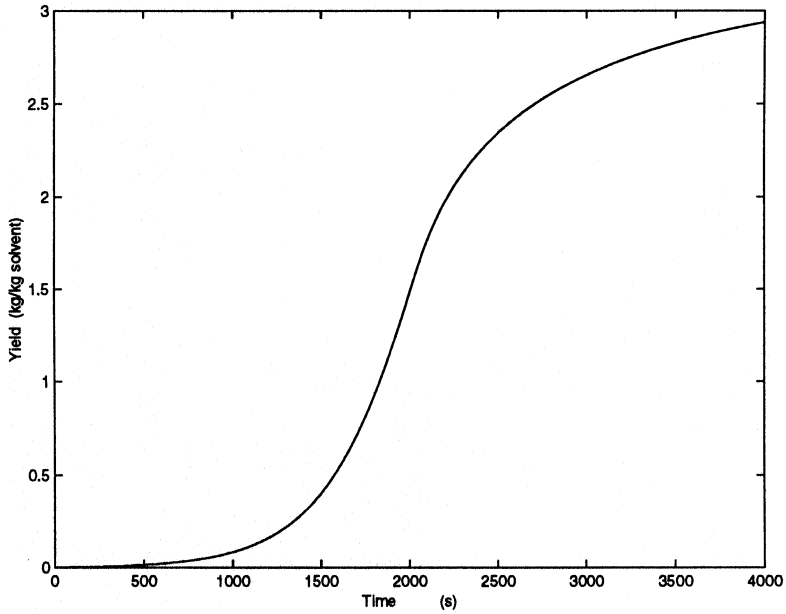

Figure 5. The product yield using the nonlinear controller with complete knowledge of state variables.

which estimates the state variables based on the measurement of crystallizer temperature and the solute concentration. The latter state variable can be measured using an on-line density meter (Redman and Rohani, 1994) or a temperature float (Wang et al., 1989). Solute concentration can also be inferred from measurements of other solution properties such as conductivity, viscosity, and refractive index.

Control with State Estimation

Two states are assumed to be measured: crystallizer temperature T and solute concentration C. In order to estimate all the states, an extended Kalman filter (Watanabe, 1992) was used. This is the nonlinear extension of the classical linear Kalman filter. As the model is continuous and the measurements are discrete, a Kalman filter in its continuous-discrete form is employed to estimate the states.

The system is now described by

$$\begin{cases} \dot{x} = f(x, u, t) + w(t) \\ y_k = h(x(t_k), k) + v_k \end{cases}, \tag{43}$$

where w and v_k are zero-mean white noises of respective covariance matrices Q and R. The extended Kalman filter in its continuous-discrete form is defined in two stages, first a continuous prediction stage for states and covariance matrix, then a discrete correction stage based on measurements where the Kalman gain is calculated and the states are updated based on the tangent linear model.

Prediction

state variables

$$\frac{d\hat{x}-}{dt} = f(\hat{x}-, u, t) \tag{44}$$

covariance estimate

$$\frac{dP^-}{dt} = FP^- + P^-F^T + Q \tag{45}$$

Correction

Kalman gain

$$K_k = P_k^- H_k^T \left[H_k P_k^{-1} H_k^T + R_k\right]^{-1} \tag{46}$$

state variables

$$\hat{x}_k^+ = \hat{x}_k^- + K_k\left[y_k - h\left(\hat{x}_k^-\right)\right] \tag{47}$$

with

$$F = \left.\frac{\partial f}{\partial x}\right|_{\hat{x}_k^-} \text{ and } H = \left.\frac{\partial h}{\partial x}\right|_{\hat{x}_k^-} \tag{48}$$

In the control law given by Equation (41), the states were replaced by their estimates. The set-point was chosen equal to 0.015 kg/kg solvent and filtered by a second-order continuous filter, as explained above. The tuning parameters of the control law in Equation (41) as well as the parameters of the PI controller are also the same as above.

The covariance matrix P was taken as diagonal with elements $P(i,i) = \hat{x}_i^2/20$ and covariance matrix Q was equal to $0.001\mathbf{I}$, where $\mathbf{I}$ is the identity matrix of convenient dimension. The temperature and solute concentration were both assumed to be affected by Gaussian noises of

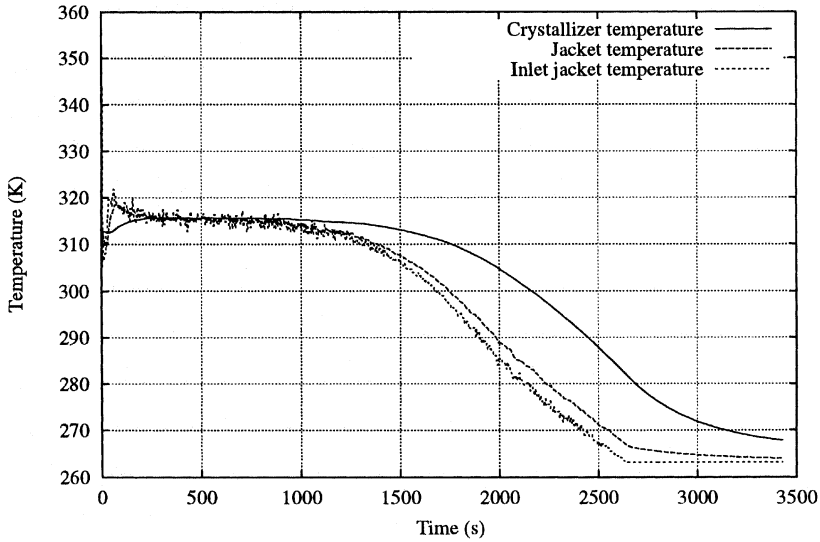

Figure 6. The supersaturation and its set-point using the nonlinear controller and the extended Kalman filter.

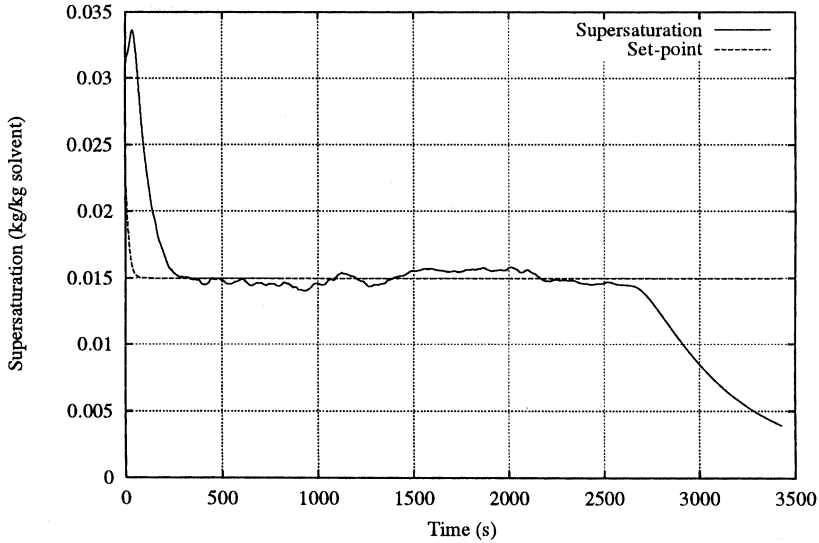

Figure 7. The crystallizer, jacket, and inlet cooling water temperatures using the nonlinear controller and the extended Kalman filter.

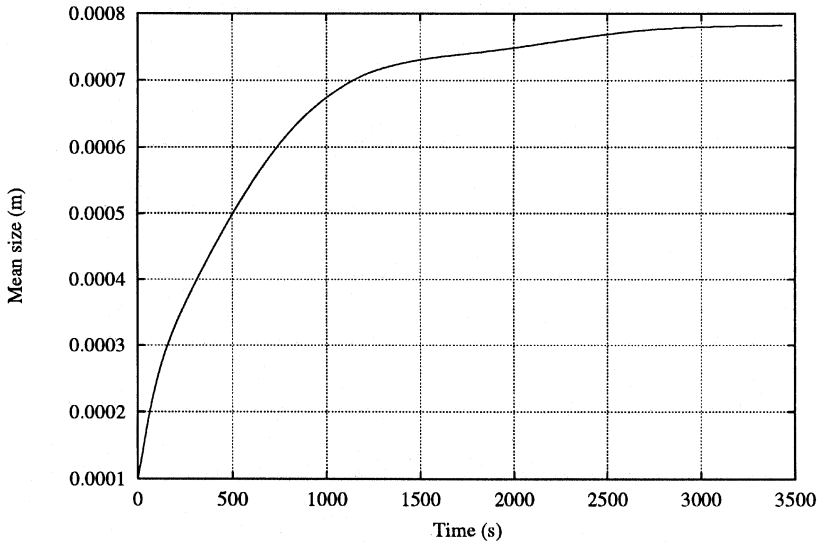

Figure 8. The terminal crystal mean-size using the nonlinear controller and the extended Kalman filter.

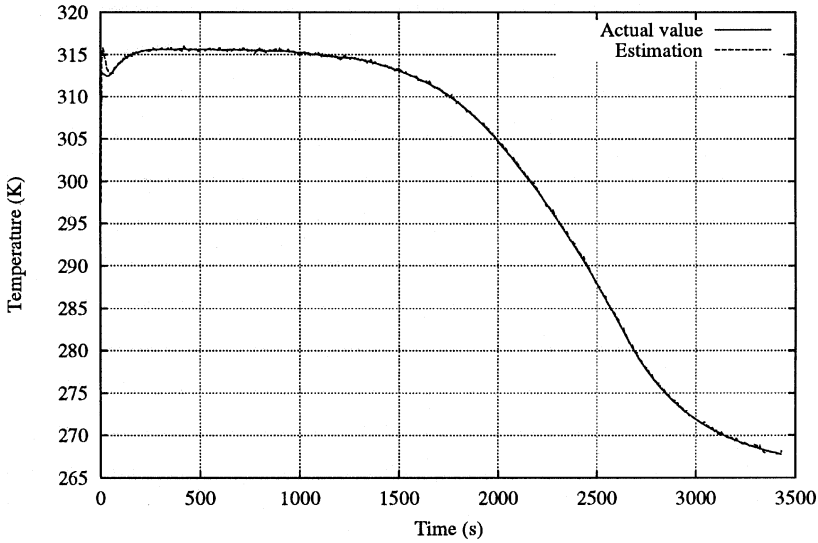

Figure 9. The crystallizer temperature and its estimate using the extended Kalman filter.

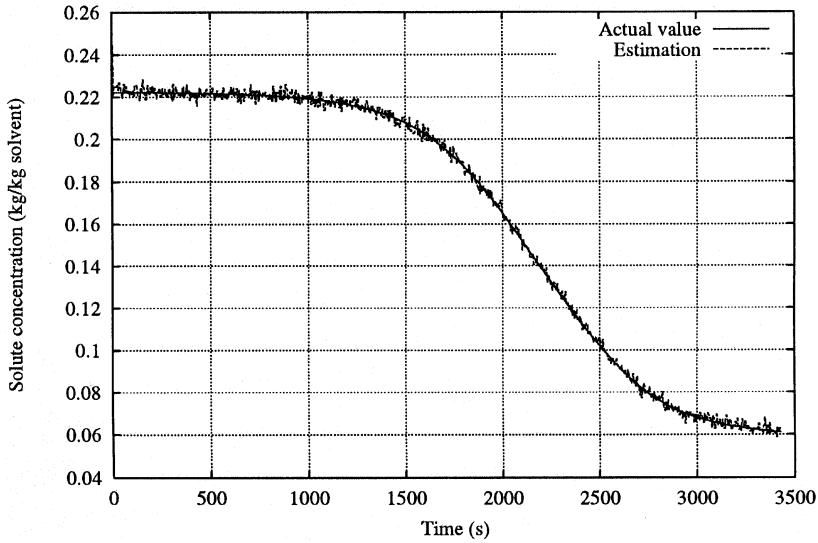

Figure 10. The solute concentration and its estimate using the extended Kalman filter.

standard deviations 0.2 and 0.002, respectively. The matrix R was diagonal with elements equal to $R(i, i) = \sigma_i^2$. Three states were estimated: the solute concentration C, the crystallizer temperature T, and the jacket temperature T_j. The other states, moments x_2 to x_6, were predicted from the model.

The general behavior of the crystallizer under the nonlinear feedback control was similar to what was observed when all the states were assumed to be perfectly known. The supersaturation (Figure 7) follows its set-point up to around 2500 s when the manipulated variable (Figure 6) saturates at its lower constraint. The crystal mean size remains almost unchanged (see Figure 8) compared to above with all states known. Figures 9 and 10 demonstrate the estimated and the measured crystallizer temperature and the solute concentration, respectively. It is clear that the Kalman filter is capable of estimating the state variables very well.

The results presented in this section demonstrate that the nonlinear controller works well even in the absence of perfect knowledge of the state variables.

CONCLUSIONS

A nonlinear geometric feedback controller was presented and applied for the control of a batch cooling crystallizer. Two cases were considered: first, it was assumed that all the state variables were perfectly known;

second, it was assumed that only two state variables, namely the crystallizer temperature and the solute concentration, were known. In both cases, the controller was capable of quickly bringing the supersaturation to its set-point and thereby eliminating the large peak in the supersaturation at the beginning of batch time. The terminal crystal mean size achieved in both cases was larger than what is reported in the literature. The nonlinear feedback control of a batch crystallizer coupled with a state-estimator based on the measurement of a limited number of easily observable state variables has advantages over more commonly practiced open-loop optimal control policies. The feedback control is capable of ensuring the desirable product mean size in the presence of external disturbances such as variations in feed quality, impurities, and mixing effects. Therefore, it is envisaged that the proposed controller with the state estimator will find applications in industry.

NOMENCLATURE

A	heat transfer area, m^2; constant matrix in Equation (33)
a_0, a_1	constants in Equation (11)
$a(z)$	defined in Equation (19)
B	nucleation rate at zero size, no/kg solvent's; constant matrix in Equation (33)
b_0, b_1	constants in Equation (10)
C	solute concentration, kg/kg solvent
c_0, c_1, c_2	constants in Equation (9)
c_p	specific heat, J/kg.K
E	activation energy, J/mol
e	error signal given by Equation (38)
F	flow rate, m^3/s, gradient vector in Equation (49), function in Equation (19)
f	function in Equation (12)
G	growth rate, m/s
g	function in Equation (12)
H	gradient vector in Equation (49)
h	total enthalpy content, J; function in Equation (12)
K	Kalman gain in Equation (47)
k_v	volumetric shape factor of crystals
L	crystal size, m; Lie derivative given in Equation (14)
L_s	size of seed crystals, m
m_k	kth moment of population density function; m^k/kg solvent
n	crystal population density function, no./kg solvent.m; number of state variables
P	covariance matrix of the Kalman filter given in Equation (46)
Q	covariance matrix of w_k in Equation (44)
$\dot{q}$	cooling rate, W
R	universal gas constant, 8.314 J/mol.K; covariance matrix of v_k in Equation (44)
r	relative order; constants in solution density given in Table I
s	Laplace operator, 1/s
T	temperature, K
t	time, s
U	overall heat transfer coefficient, $W/m^2.K$
u	vector of manipulated variables

V	volume, m^3
v	external input given in Equation (26), white measurement noise in Equation (44)
W	mass of solvent, kg
w	white process noise in Equation (44)
x	state vector
y	output vector
z	transformed variables defined by Equation (16)

Greek Letters

α	constants in Equation (38)
ΔC	supersaturation, kg/kg solvent
ΔH	heat of crystallization, J/kg crystals
ϕ	auxiliary variables defined in Equation (17)
γ	function defined in Equation (29)
ξ	defined in Equation (35)
η	defined in Equation (36)
ρ	density, kg/m^3; constant in Equation (38)

Subscripts

B	nucleation
C	crystals
G	growth
i	inlet
j	jacket
k	kth moment, sampling instant in Equation (44)
o	outlet
R	controller set-point
ref	reference temperature
s	solution
w	water
0	initial condition

Superscripts

*	saturation condition
^	estimate

REFERENCES

Akoglu, K., Tavare, N. S. and Garside, J. (1984). Dynamic simulation of a non-isothermal MSMPR crystallizer, *Chem. Eng. Comm.* **29**, 353–367.

Hirschorn, R. M. (1979). Invertibility of nonlinear control systems, *SIAM J. Control Optim.* **17**(2), 289.

Isidori, A. (1995). *Nonlinear Control Systems*, Springer Verlag, Berlin.

Jones, A. G. and Chianese, A. (1987). Fines destruction during batch crystallization, *Chem. Eng. Comm.* **62**, 5–16.

Jones, A. G. and Mullin, J. W. (1974). Programmed cooling crystallization of potassium sulfate solutions, *Chem. Eng. Sci.* **29**, 105–118.

Khalil, H. K. (1996). *Nonlinear Systems*, Prentice Hall, Upper Saddle River, NJ.

Levine, W. S. (Ed.). (1996). *The Control Handbook*, CRC Press, Boca Raton, FL.

Mayrhofer, B. and Nyvlt, J. (1988). Programmed cooling of batch crystallizers, *Chem. Eng. Process* **24**, 217–220.

Miller, S. M. and Rawlings, J. B. (1994). Model identification and control strategies for batch cooling crystallizers, *AIChE J.* **10**(8), 1312–1327.

Nijmeijer, H. and van der-Schaft, A. (1990). *Nonlinear Dynamical Control Systems*. Springer-Verlag, New York.

Redman, T. and Rohani, S. (1994). One-line determination of supersaturation of a KCl-NaCl aqueous solution based on density measurement, *Can. J. Chem. Eng.* **72**, 64–71.

Rohani, S. and Bourne, J. R. (1990). Self-tuning control of crystal size distribution in a cooling batch crystallizer, *Chem. Eng. Sci.* **45**(12), 3457–3466.

Rohani, S., Tavare, N. S. and Garside, J. (1990). Control of crystal size distribution in a batch cooling crystallizer, *Can. J. Chem. Eng.* **68**, 260–267.

Sheik, A. Y. and Jones, A. G. (1997). Crystallization process optimization via a revised machine learning methodology, *AIChE J.* **43**(6), 1448–1457.

Slotine, J. J. E. and Li, W. (1991). *Applied Nonlinear Control*, Prentice Hall, Englewood Cliffs, NJ.

Wang, Z.-K., Zeng, Q.-S. and Qian, R.-Y. (1989). Precise determination of supersaturation by temperature float method, *AIChE J.* **35**, 679–682.

Watanabe, K. (1992). *Adaptive Estimation and Control*, Prentice Hall, New York.